02 May 2013, 4:00 pm - 6:00 pm

# 3D FEM Modelling of a Deep Excavation Case Considering Small-Strain Stiffness of Soil and Thermal Shrinkage of Concrete

Yuepeng Dong
*University Of Oxford, United Kingdom*

Harvey Burd
*University Of Oxford, United Kingdom*

Guy Houlsby
*University Of Oxford, United Kingdom*

Zhonghua Xu
*East China Architectural Design & Research Institute, China*

Commemorate the Legacy of Ralph B. Peck
April 29 - May 4, 2013 CHICAGO
Seventh International Conference on
Case Histories in Geotechnical Engineering
and Symposium in Honor of Clyde Baker

# 3D FEM MODELLING OF A DEEP EXCAVATION CASE HISTORY CONSIDERING SMALL-STRAIN STIFFNESS OF SOIL AND THERMAL SHRINKAGE OF CONCRETE

**Yuepeng Dong, Harvey Burd, Guy Houlsby**
Department of Engineering Science, University of Oxford, Oxford, U.K. OX1 3PJ

**Zhonghua Xu**
East China Architectural Design & Research Institute, Shanghai, P.R. China, 200002

ABSTRACT

A typical top-down deep excavation project in Shanghai was carefully monitored during the construction process. This case history was back-analysed with a complex 3D FEM numerical model in ABAQUS to investigate the influence of different modelling procedures. The model considered the detailed construction procedures and structural information. The calculations included the small-strain stiffness of the soil and thermal shrinkage of the concrete beams and slabs. The small-strain stiffness is modelled with a multi-surface soil model developed at Oxford which has been implemented into ABAQUS. The diaphragm wall was modelled as an anisotropic linear elastic material to represent the effect of the joints in the wall. The beam and slabs were modelled as a linear elastic material and including the shrinkage of concrete. The numerical results captured the main excavation behavior and agreed well with the field measurements. Two sets of calculations were conducted to investigate the influence of soil models and thermal shrinkage on the computed excavation behaviour. The results showed that small-strain soil stiffness is crucial to capture the excavation behavior and the thermal shrinkage of concrete should not be neglected in deep excavation problem.

## INTRODUCTION

Deep excavations are frequently used in congested cities to provide underground space. However, the construction of deep excavations will inevitably induce ground movements and structure deformations which may cause damage to adjacent buildings and services. The prediction of ground movements around deep excavations is not straightforward because they are complicated and critically dependent on both the ground conditions and the method of construction.

In an effort to better understand the behaviour of deep excavations, a number of case histories have been published (Finno, Atmatzidis et al. 1989; Ou, Liao et al. 1998; Ou, Liao et al. 2000; Finno and Bryson 2002; Liu, Ng et al. 2005; Ou, Hsieh et al. 2010; Liu, Jiang et al. 2011). Although those cases vary a lot from one to another, they provide valuable resources for back analysis.

Numerical modelling is a powerful tool for the analysis of deep excavations. However, it is not routinely used for design because FEM analysis is complicated and time-consuming, and requires advanced skills of experienced engineers. There exists some related publications on both 2D and 3D FEM modelling (Simpson 1992; St. John, Potts et al. 1993; Whittle, Hashash et al. 1993; Hashash and Whittle 1996; Ou, Chiou et al. 1996; Zdravkovic, Potts et al. 2005; Hashash, Song et al. 2011), but the modelling was largely simplified and therefore missed a number of important details. Research has showed that small-strain stiffness is vital important to capture the excavation behaviour (Simpson 1992;Whittle, Hashash et al. 1993; Zdravkovic, Potts et al. 2005). But the thermal shrinkage of concrete struts due to variation of the ambient temperature and curing process is seldom considered in the previous analysis, which is evident and non-negligible (Dong, Burd et al. 2012).

In this paper, a top-down deep excavation case history is analysed with a 3D FEM model in ABAQUS, and the influence of soil models and the thermal shrinkage of concrete is investigated.

## CASE HISTORY DESCRIPTION

### General Description

Shanghai Xingye bank building, as shown in Fig. 1, is a 82.5m high-rise building with a 3-floor basement. The main building is reinforced concrete frame-shear resistance wall system, with

pile-raft foundation (Wang and Wang 2007; Xu 2007). The piles are bored piles, 0.9m in diameter, and around 60m in length. The whole project covers an area of about 7856m², and the excavation area is around 6200m². The excavation is 14.2*m* deep on the west side, and 12.2m deep on the east side. The project is situated in the downtown area of Shanghai, surrounded by 15 densely distributed buildings of which 8 are historical buildings with high protection standard, as well as some aged pipelines.

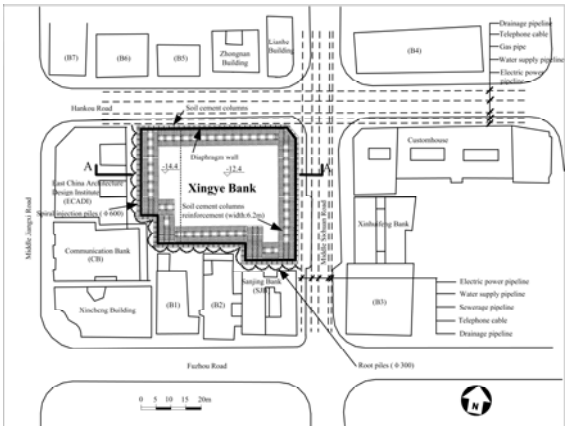


*Fig. 1, Plan view of the deep excavation*

Fig. 2 shows the section view of the excavation and the supporting structures. The excavation is retained by a 1m thick diaphragm wall which is supported by horizontal beams and slabs, as shown in Fig. 3.

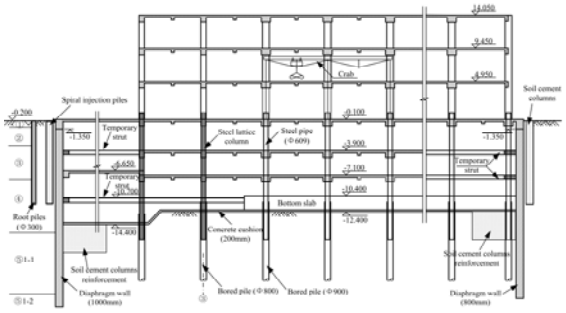


*Fig. 2, Section view of A-A*

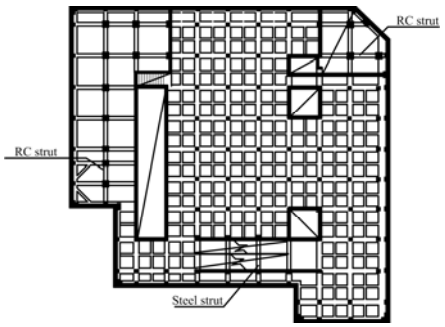


*Fig. 3, First floor underground beams and slabs*

The 60m deep piles provide vertical support to the whole structure. The excavation is constructed with top-down methods, and the above buildings can be constructed to the 3rd floor at the same time with the excavation. This excavation was carefully measured during construction.

Geotechnical Conditions and Soil Properties

The city of Shanghai is situated at proximately 70km from the sea shore, in the large coastal plain limited by the East China Sea and the Yangtze River which is designated as the 'Yangtze River Delta'. The subsoil of Shanghai is composed of Quaternary sediments of the Yangtze River estuary which consist of clay, loam, silt and sand, the different deposits being the final result of the variation from an estuarine to fluviatile sedimentation process (Dassargues, Biver et al. 1991). The elevation of the ground surface is typically from 2.2m to 4.8m above sea level (Xu, Shen et al. 2009).

According to the site investigation report, the site is on a flat coastal plain, with ground elevation between 4.80m to 3.87m, and ground water table 0.5 to 1m below the ground surface. Based on the differences of soil characteristics, physical and mechanical properties, the soil profile can be divided into 7 sub layers, as shown in Fig. 4, with the corresponding soil properties.

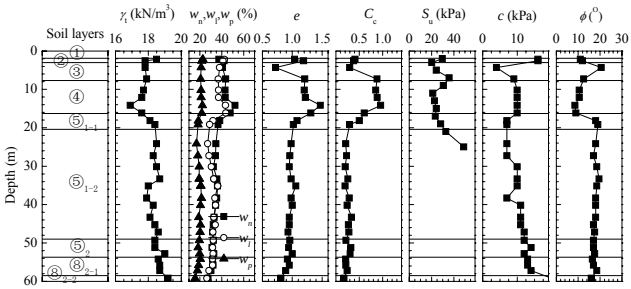


Note: $\gamma_t$=unit weight, $w_n$=water content, $w_p$=plastic limit, $w_l$=liquid limit, e=void ratio, $c_c$=compressive index, $s_u$= field vane shear strength, c=cohesive strength, φ=internal friction angle.

*Fig. 4, Geotechnical profile and soil properties*

Some of the soil parameters for numerical modelling are derived from Fig. 4. The unit weight generally increases with depth, but it is convenient to take its average value, roughly 18.5kN/m³. For the undrained shear strength $s_u$, the data in Fig. 4 is not sufficient for numerical modelling. Therefore, a more complete $S_u$ profile is collected from Dassargues, Biver et al.(1991), and Equation (1) is derived by linearizing the data.

$$s_u = (20 + 2z)\text{kPa} \qquad (1)$$

The small-stain stiffness of the soil is missing from the site investigation report, but it could be collected from publications about Shanghai clay. Stiffness at very small strain $G_0$ can be measured using dynamic methods. Cai, Zhou et al.

(2000) studied the dynamic characters of typical Shanghai clay and silt through several types of laboratory dynamic tests, and the value of $G_0$ is citied and generalised as Equation (2).

$$G_0 = (20 + 2z)\ \text{MPa} \qquad (2)$$

The small-strain stiffness properties are taken from Zhang and Shi (2008), and shown in Equation (3).

$$\frac{G}{G_{0,max}} = \frac{1}{1 + 9.2(\frac{\varepsilon_s}{0.475\%})^{1.34}} \qquad (3)$$

Based on Equation (3), a normalised curve is plotted in Fig. 5, in which both the stiffness $G$ and shear strain $\gamma$ are normalised and it is believed that it has advantages in physical meaning.

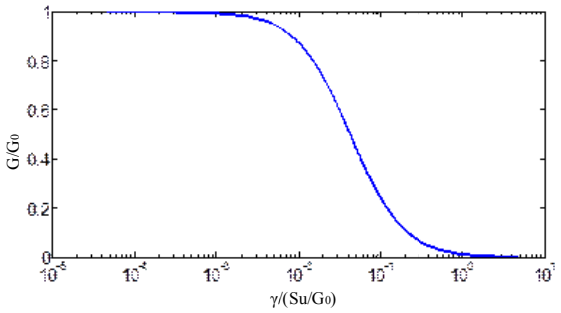


*Fig. 5, Normalized S-shaped curves.*

Instrumentations

Due to the high environmental protection standard, a careful and comprehensive field measurement was carried out during the construction process to monitor the performance of the deep excavation. The detailed instrumentation layout is shown in Fig. 6.

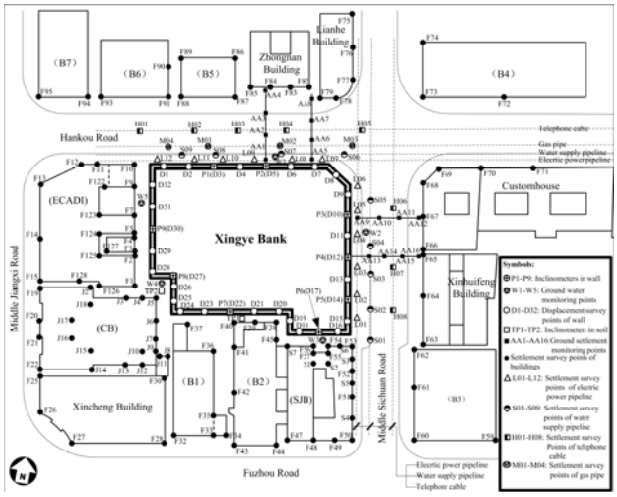


*Fig. 6, Layout of instrumentation at the construction site*

The observed items include:

1. Lateral wall displacement, $P1{\sim}P9$;
2. Vertical and horizontal displacement at top of the diaphragm wall, $D1{\sim}D32$;
3. Lateral earth displacement outside the excavation, $TP1{\sim}TP2$.
4. Ground water level, $W1{\sim}W5$;
5. Ground settlement outside the excavation $AA1{\sim}AA4$, $AA5{\sim}AA8$, $AA91{\sim}P12$, $P13{\sim}P16$;
6. Settlement of pipelines, including electrical power pipelines ($L01{\sim}L12$), cast-iron water-supply pipelines ($S01{\sim}S09$), gas pipelines ($M01{\sim}M04$), and telephone cable pipelines ($H01{\sim}H08$);
7. Building settlements;

## FEM MODEL AND INPUT PARAMETERS

Model Description

The FEM model includes the detailed information of structures and the top-down construction procedures. Fig. 7 shows the excavation geometry and boundary conditions.

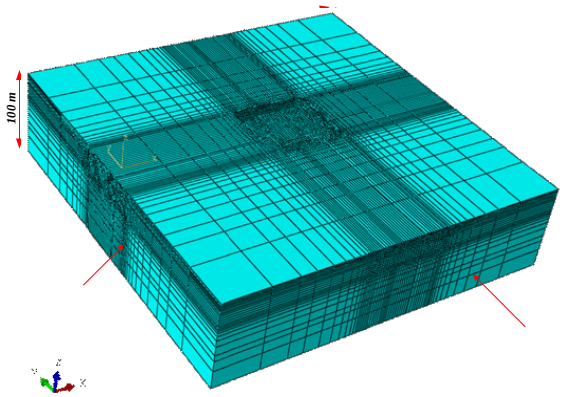


*Fig. 7, Soil mesh and boundary conditions*

The mesh of the diaphragm wall and support system is shown in Fig. 8 and Fig. 9.

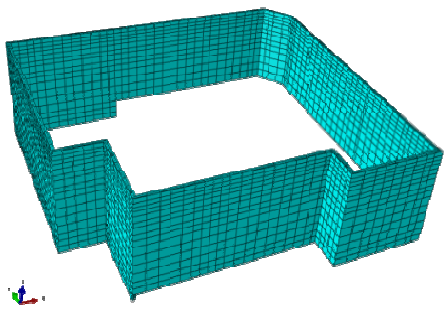

*Fig. 8, Diaphragm wall geometry and mesh*

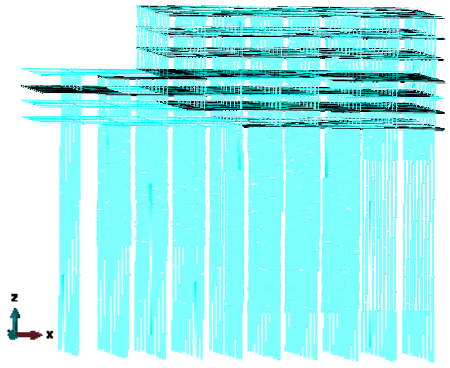

*Fig. 9, Supporting system and superstructures*

The soil and the diaphragm wall are modelled with 8-noded hexahedral elements. However, shell elements are also very popular to model the diaphragm wall because it can output the internal force and bending moment directly. But it has been proven that it tends to overestimate the wall deflection and ground settlement because it misses the beneficial bending moment caused by shear stress on the interface of the wall about the wall centre line due to its no-thickness in geometry in FEM (Dong, Burd et al. 2012). The piles and beams are modelled with 2-noded 3D beam elements. The slabs are modelled with 4-noded quadrilateral shell elements. This model has totally 102,036 elements and 116,756 nodes. Quadratic elements are tried, and the results are almost same with the linear elements but it takes much longer time to run.

The excavation is modeled in undrained conditions. Consolidation and dewatering is not considered here. The calculations are conducted on the Oxford supercomputer.

Input Parameters

The soil is modelled with a multi-surface soil model (Houlsby 1999) developed at Oxford which has been implemented into ABAQUS through a subroutine UMAT (Dong 2011), to consider the small-strain stiffness of the soil. The nested yield surface model, formulated within the framework of work-hardening plasticity theory, takes into account the non-linear behaviour of soil at small strains, and also includes effects such as hysteresis and dependence of stiffness on recent history. Non-linearity of the small-strain response is achieved using a number of nested yield surfaces of the same shape as the outer fixed surface, as shown in Fig. 10.

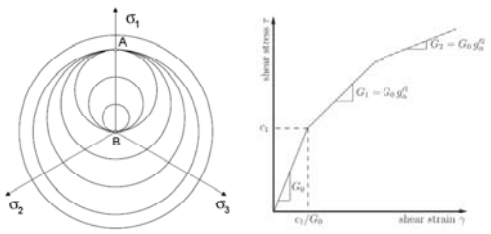


*Fig. 10, Nested yield surface model*

The stiffness at very small strain $G_0$ and the undrained strength $S_u$ increase linearly with depth, as shown in Equation (1) and Equation (2) respectively. The small-strain stiffness parameters for the nested yield surface model are derived from Fig. 5. To investigate the influence of soil models, two built-in soil models in ABAQUS, linear elastic and the Tresca soil model, are also used.

The diaphragm wall is modelled with anisotropic elastic properties to consider the joints in the wall (Zdravkovic, Potts et al. 2005). The out-of-plane and in-plane stiffness ratio $E_{out}/E_{in} = 0.1$ is adopted based on some back analyses of this case history. The elastic properties of concrete are $E = 30GPa, v = 0.2$.

In most analyses from existing publications, beams and slabs are modelled as linear elastic material with 20% reduction of the design stiffness to consider open access, shrinkage, cracks, and workmanship of the construction (Simpson 1992; St. John, Potts et al. 1993). Although simple, it has no physical meaning. In the analyses here, they are modelled as linear elastic material but including the thermal contraction which is evident due to temperature change during concrete curing process and ambient temperature variation(Whittle, Hashash et al. 1993; Boone and Crawford 2000; Hashash, Marulanda et al. 2003). The Coefficient of Thermal Expansion (CTE) is$10 \times 10^{-6}/℃$, associated with temperature change $\Delta T = -35℃$ which is also based on back analysis.

## ANALYSIS STRATEGIES AND CALCULATIONS

The strategy of the analyses is to focus on one central analysis which is believed to consider every important aspect of the problem and the result agrees best with the field data. All the other analyses are grouped and compared with the central analysis and field data to investigate their influence on the excavation behaviour.

The central analysis is conducted based on the back analysis of the case history to obtain a group of optimised parameters. And in other calculations, only one parameter is changed each time. The run ID and description are shown in Table 1 and Table 2. The numerical results are shown in the next sections, as well as the field data.

The focus of the calculations is to investigate the influence of soil models and thermal shrinkage of concrete on the excavation behaviour. Therefore, the calculations are divided into two groups and the results are compared in each group.

## RESULTS INTEPRETATION

There is a large amount of data from both numerical modelling and field measurements, but it is not appropriate to present all of them here. Therefore, only some selected data

from the field measurements is compared with numerical results, as shown in Fig. 11.

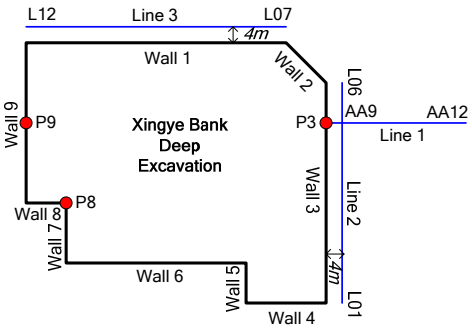


*Fig. 11, Field instrumentations*

The comparison is focused on one wall deflection at wall centre (P9) and one at wall corner (P8), and the ground settlement along Line 1, Line 2 and Line 3. And it is believed that the data can reflect a complete picture of the excavation behaviour.

In this section, results from two sets of calculations are presented, in order to demonstrate the influence of soil models and thermal shrinkage of concrete on the excavation behaviour.

Influence of soil models

To investigate the effect of different soil models, besides the central analysis which considers the small-strain stiffness of the soil using the nested yield surface model, three other runs are conducted with simpler soil models, as shown in Table 1. The results are compared with the filed data.

Table 1 FEM Runs and Description

| Run ID | Description |
|---|---|
| Central analysis | Soil Model: Nested-yield surface model, stiffness and strength increase linearly with depth;<br>Wall Model: anisotropic elastic, $E_{out}/E_{in} = 0.1$,<br>Beams and Slabs: elastic, $\alpha = 10 \times 10^{-6}/°C$, $\Delta T = -35°C$ |
| SME | Same as central analysis except that the soil model is linear elastic with constant soil parameters<br>$G = 9MPa, \mu = 0.49$ |
| SMTC | Same as central analysis except that the soil model is Tresca with constant soil parameters;<br>$G = 9MPa, \mu = 0.49, S_u = 50kPa$ |
| SMTV | Same as central analysis except that the soil model is Tresca and soil stiffness and strength increases linearly with depth;<br>$G = 180S_u, \mu = 0.49, S_u = (20 + 2z)kPa$ |

To make these analyses comparable, some assumptions of the soil parameters are adopted. For linear elastic analysis and Tresca soil model with constant soil properties, the stiffness G is adopted as $G_{50}$ (stiffness at 50% of the shear strength) from Fig. 5, and the strength $S_u$ is taken at the depth of 15m, roughly half of the wall depth. For Tresca soil model with variable soil parameters, $G_{50} \approx 0.180G_0$, and $G_0/S_u = 1000$ is used here, so $G_{50} \approx 180S_u$.

The results of calculations in Table 1 are shown in Fig. 12 - Fig. 16, together with the field data.

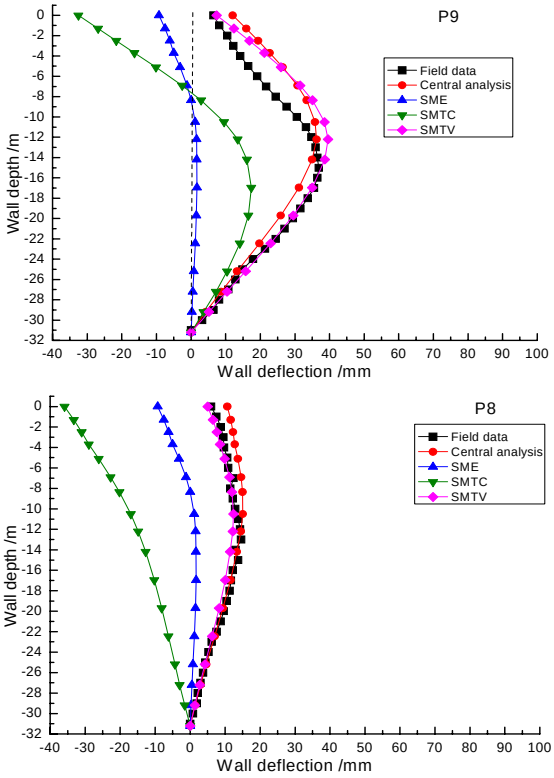


*Fig. 12, Wall deflection at P9 and P8*

From Fig. 12, it is shown that the central analysis agrees well with the field data. Tresca soil model with variable stiffness and strength soil parameters could also capture the pattern of wall deflection very well. But the linear elastic model and Tresca soil models with constant soil parameters perform rather poorly, and therefore they are not suitable to use for prediction purposes.

The ground settlement along Line 1 is shown in Fig. 13. Again, the results indicate that the central analysis with the nested yield surface model captures the ground movement very well because it considers the small-strain stiffness of the soil. But the other three, even the Tresca soil model with variable soil properties which could predict the wall deflection well, fail to produce both the pattern and magnitude of the ground movement. For the linear elastic and Tresca soil model, the ground movement around the excavation is upward which contradicts with the field data. If they were used for the prediction of the adjacent infrastructures around the excavation, the result would be misleading. Therefore, in order to get reasonable results for ground movement, the small-

strain stiffness must be considered in the analysis.

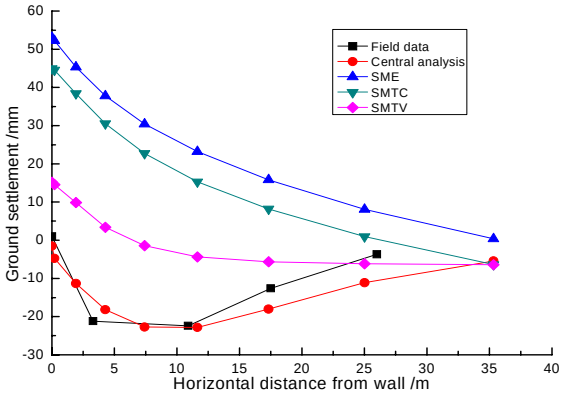


*Fig. 13, Ground settlements along Line 1*

The ground settlement along Line 2 and Line 3 is shown in Fig. 14. Again, it demonstrates that when the small-strain stiffness of soil is considered the numerical result can capture the ground settlement. Otherwise, the results are disappointing when compared with the field data.

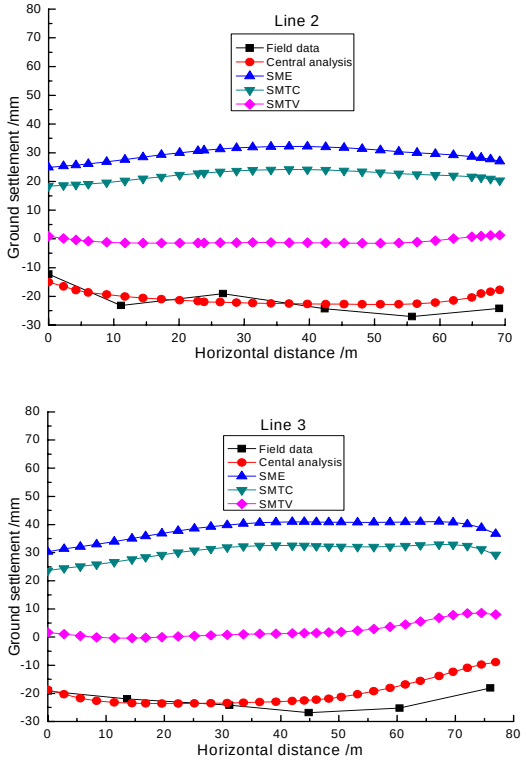


*Fig. 14, Ground settlements along Line 2 and Line 3*

Influence of concrete thermal shrinkage

To investigate the influence of thermal contraction of concrete and different temperature change on the excavation behaviour, results from another two runs, as shown in Table 2, are compared with the central analysis as well as the field data. The results are presented as below.

Table 2 FEM runs and description

| Run ID | Description |
|---|---|
| Central analysis | Soil Model: Nested-yield surface model, stiffness and strength increase linearly with depth;<br>Wall Model: anisotropic elastic, $E_{out}/E_{in} = 0.1$,<br>Beams and Slabs: elastic, $\alpha = 10 \times 10^{-6}/℃$ , $\Delta T = -35℃$ |
| ANE1T30 | Same as central analysis except $\Delta T = -30℃$ |
| ANE1T40 | Same as central analysis except $\Delta T = -40℃$ |

The results of the analyses listed in Table 2 are shown in Fig. 15~Fig. 16, together with the field data.

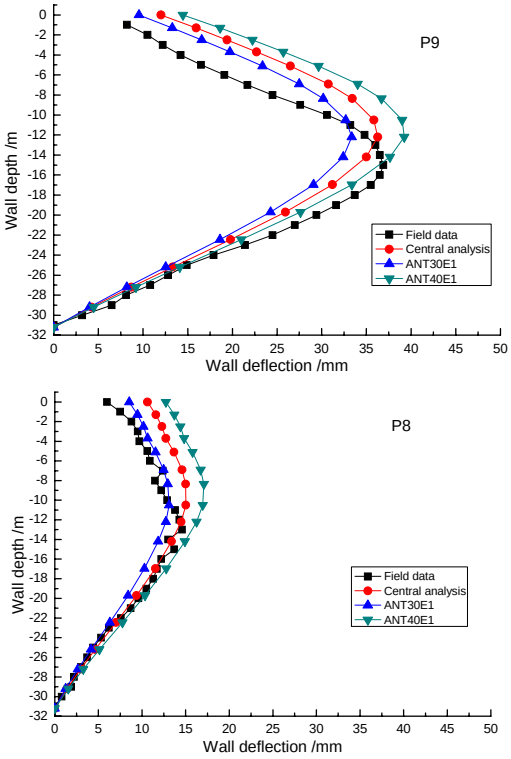


*Fig. 15 Wall deflection at P9 and P8*

The results show that the wall deflection is sensitive to temperature change inside the concrete during curing process. When the concrete cools down by 5℃, the beams and slabs shrink and the wall deflections increase around 3mm. But the wall deflection increment at P8 is slightly smaller than that at P9 due to the corner effect. Therefore, this effect should not be neglected in the analyses.

The ground settlement behind the wall along Line 1 is plotted in Fig.16, together with the field data.

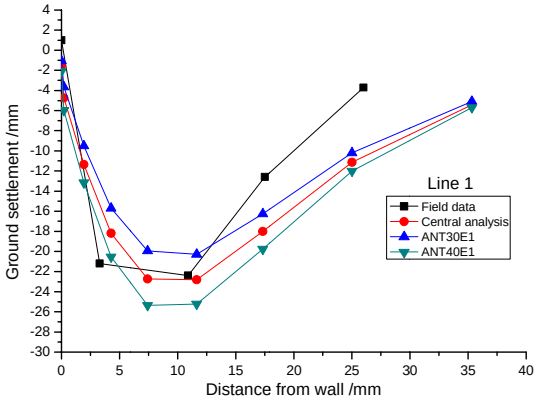


*Fig. 16, Ground settlements along Line 1*

The results shows that the ground settlement increases by around 3mm when the temperature of concrete reduces 5℃, which is accompanied by the increase of the wall deflection.

The ground settlements behind the wall along Line 2 and Line 3 are shown in Fig. 17, together with the field data.

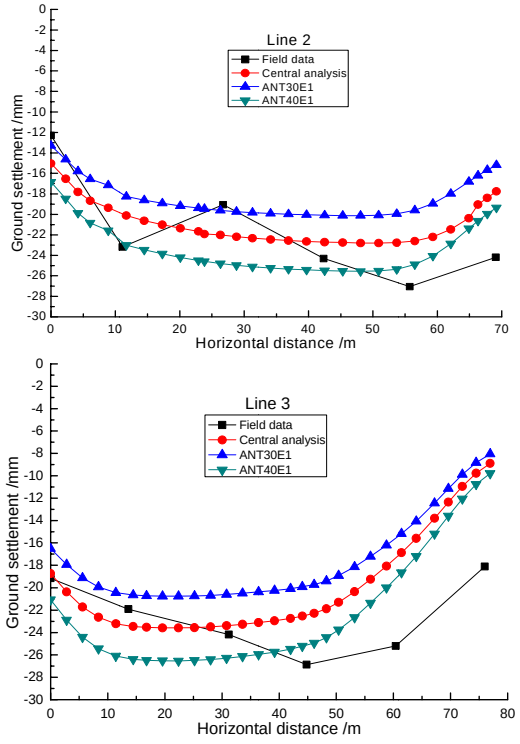


*Fig. 17, Ground settlements along Line 2 and Line 3*

Fig. 17 is consistent with the ground settlement along Line 1 and indicates that ground settlement behind the wall is sensitive to thermal contraction of concrete. But the settlement change behind the wall corner is smaller than that behind the wall centre.

CONTOUR DISPLAY

The displacement contours from the central analysis are shown below, from which the displacement distribution of soils and structures is clearly seen.

The ground vertical displacement contour is displayed in Fig. 18.

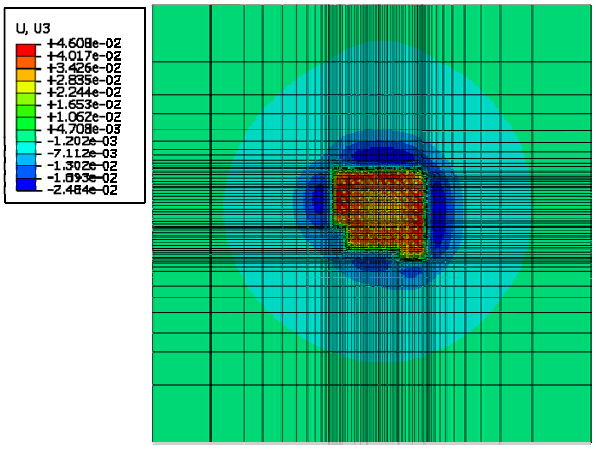


*Fig. 18, Ground vertical displacement (m)*

The largest ground settlement is concentrated behind the wall centre around the excavation, while the settlement is smaller around the corner due to the soil arching effect. The longer the wall, the larger is the ground settlement area. The basal heave is also evident inside the excavation due to stress relief. The soil displacement decreases as the distance from excavation increases, and the displacement around the boundary is nearly zero.

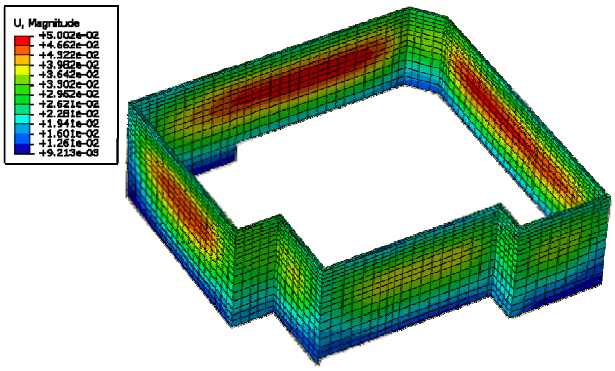


*Fig. 19, Wall deflection (m)*

As shown in Fig.19, the largest wall deflection is concentrated at the wall centre area close the excavation depth, while the deflection at the corner is smaller due to the corner effect. The shape of the diaphragm wall also affects the wall deflection.

The displacement at the wall bottom is not trivial, although in field measurement it is usually assumed that the wall is fixed at the toe. This assumption depends on the geological conditions and wall depth.

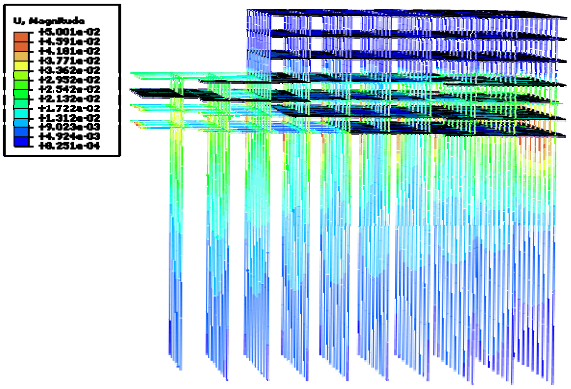

*Fig. 20, Displacement distribution of the supporting system*

Fig. 20 shows the deformation of the supporting system. It is useful to compare with the field measurement in order to understand the performance of the structure. The internal force and bending moment can also be obtained directly, which is beneficial for design purposes.

## CONCLUSIONS

The 3D numerical analysis is a true reality in deep excavation problems, which could consider details of irregular geometries, non-linear material properties and staged construction procedures. From the numerical results, the spatial distribution of displacements and stresses is clearly presented, which could provide rather useful information for research, design and construction.

In order to capture the main excavation behaviour, besides the detailed structure and construction information, the 3D FEM model should consider the following two aspects:

1. The small-strain stiffness of the soil should be considered to get realistic wall deflection ground movement. Tresca soil model with variable stiffness and strength properties could predict the pattern of wall deflection, but its prediction of the ground movement is rather poor. The Tresca soil model with constant properties and linear elastic model are not suitable to use.
2. Concrete thermal contraction induced by temperature change during the curing process and ambient temperature variation is non-negligible in excavation problems.

## ACKNOWLEDGEMENT

The scholarship from China Scholarship Council is acknowledged, which is crucial for my study in Oxford. The case history is from Shanghai Jiao Tong University, China. The calculations were conducted on Oxford supercomputer

## REFERENCES

Boone, S. J. and A. M. Crawford (2000). "Braced excavations: Temperature, elastic modulus, and strut loads." Journal of Geotechnical and Geoenvironmental Engineering **126**(10): 870-881.

Cai, H., J. Zhou, et al. (2000). "Plastoelastic response of horizontally layered sites under multi-directional earthquake shaking." Tongji Daxue Xuebao/Journal of Tongji University **28**(2): 177-182.

Dassargues, A., P. Biver, et al. (1991). "Geotechnical properties of the Quaternary sediments in Shanghai." Engineering Geology **31**(1): 71-90.

Dong, Y. P. (2011). Numerical Modelling of Ground Movement and Structure Deformation Induced by Excavation. PRS first year transfer report. Oxford, Department of Engineering Science, University of Oxford.

Dong, Y. P., H. J. Burd, et al. (2012). 3D FEM modelling of a deep excavation case history considering small-strain stiffness of soil and thermal contraction of concrete. Young Geotechnical Engineers's Symposium 2012, University of Leeds.

Finno, R. J., D. K. Atmatzidis, et al. (1989). "Observed performance of a deep excavation in clay." Journal of geotechnical engineering **115**(8): 1045-1064.

Finno, R. J. and L. S. Bryson (2002). "Response of building adjacent to stiff excavation support system in soft clay." Journal of Performance of Constructed Facilities **16**(1): 10-20.

Hashash, Y. M. A., C. Marulanda, et al. (2003). "Temperature correction and strut loads in Central Artery excavations." Journal of Geotechnical and Geoenvironmental Engineering **129**(6): 495-505.

Hashash, Y. M. A., H. Song, et al. (2011). "Three-dimensional inverse analyses of a deep excavation in Chicago clays." International Journal for Numerical and Analytical Methods in Geomechanics **35**(9): 1059-1075.

Hashash, Y. M. A. and A. J. Whittle (1996). "Ground movement prediction for deep excavations in soft clay." Journal of Geotechnical and Geoenvironmental Engineering **122**(6): 474-486.

Houlsby, G. T. (1999). A model for the variable stiffness of undrained clay. Proceedings of the International Symposium on Pre-Failure Deformations of Soil, Torino.

Liu, G. B., R. J. Jiang, et al. (2011). "Deformation characteristics of a 38 M deep excavation in soft clay." Canadian Geotechnical Journal **48**(12): 1817-1828.

Liu, G. B., C. W. W. Ng, et al. (2005). "Observed performance of a deep multistrutted excavation in Shanghai soft clays." Journal of Geotechnical and Geoenvironmental Engineering **131**(8): 1004-1013.

Ou, C. Y., D. C. Chiou, et al. (1996). "Three-dimensional finite element analysis of deep excavations." Journal of Geotechnical and Geoenvironmental Engineering **122**(5): 337-345.

Ou, C. Y., P. G. Hsieh, et al. (2010). "Performance of excavations with cross walls." Journal of Geotechnical and Geoenvironmental Engineering **137**(1): 94-104.

Ou, C. Y., J. T. Liao, et al. (2000). "Building response and ground movements induced by a deep excavation." Geotechnique **50**(3): 209-220.

Ou, C. Y., J. T. Liao, et al. (1998). "Performance of diaphragm wall constructed using top-down method." Journal of Geotechnical and Geoenvironmental Engineering **124**(9): 798-808.

Simpson, B. (1992). "Retaining structures: displacement and design." Geotechnique **42**(4): 541-576.

St. John, H. D., D. M. Potts, et al. (1993). "Prediction and performance of ground response due to construction of a deep basement at 60 Victoria Embankment." Predictive soil mechanics. Proc. of the Wroth memorial symposium, Oxford, 1992: 581-608.

Wang, W. D. and J. H. Wang (2007). Design, analysis and case histories of deep excavations supported by permanent structures. Beijing, China Architecture & Building Press.

Whittle, A. J., Y. M. A. Hashash, et al. (1993). "Analysis of deep excavation in Boston." Journal of Geotechnical Engineering - ASCE **119**(1): 69-90.

Xu, Y.-S., S.-L. Shen, et al. (2009). "Geological and hydrogeological environment in Shanghai with geohazards to construction and maintenance of infrastructures." Engineering Geology **109**(3–4): 241-254.

Xu, Z. H. (2007). Deformation Behaviour of Deep Excavations supported by Permanent Structure in Shanghai Soft Deposit. PhD, Shanghai Jiao Tong University, China.

Zdravkovic, L., D. M. Potts, et al. (2005). "Modelling of a 3D excavation in finite element analysis." Geotechnique **55**(7): 497-513.

Zhang, P. S. and J. Y. Shi (2008). "Effect of stress path circumgyration on shear modulus under small strain and initial stress state." Yantu Gongcheng Xuebao/Chinese Journal of Geotechnical Engineering **30**(3): 379-383.